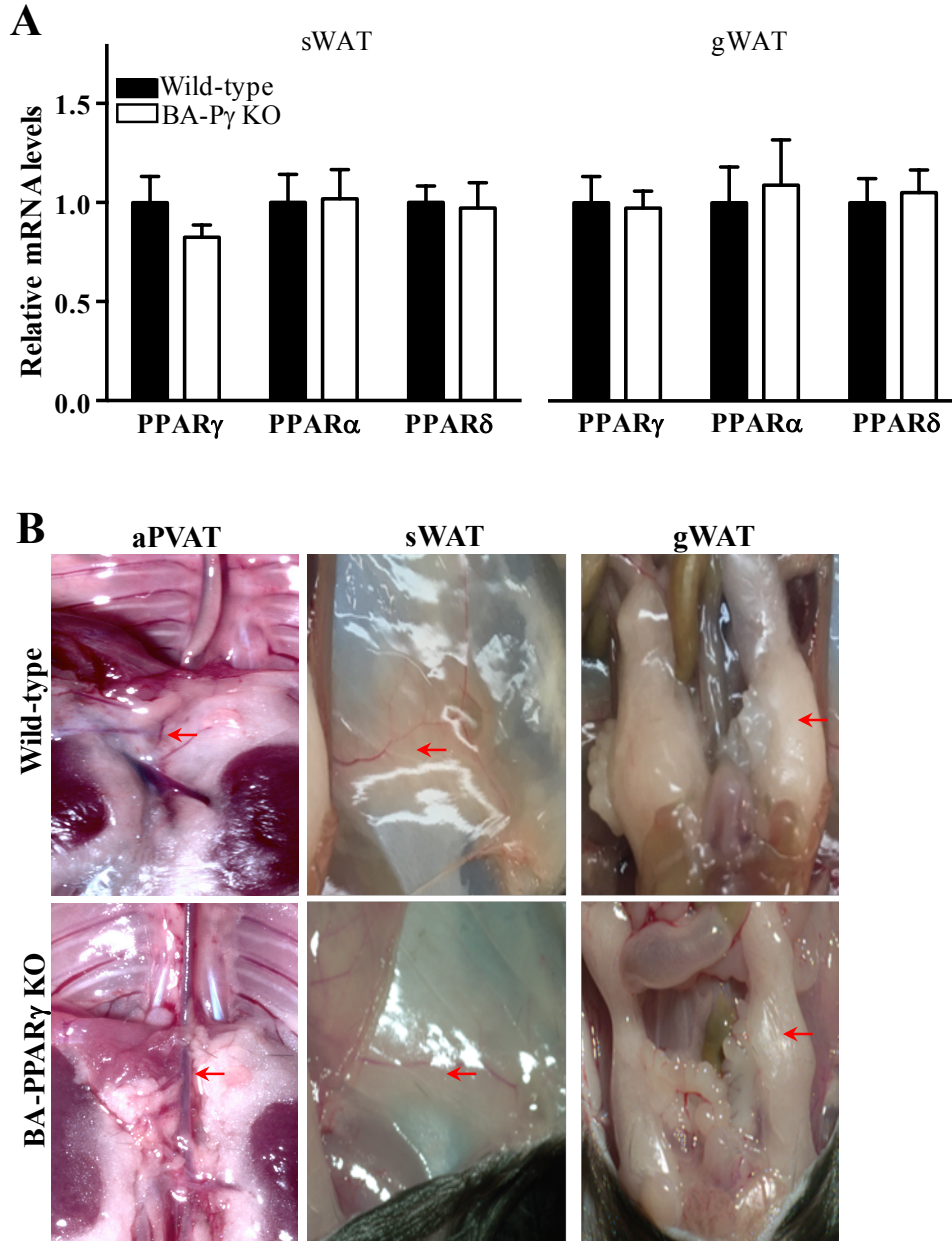
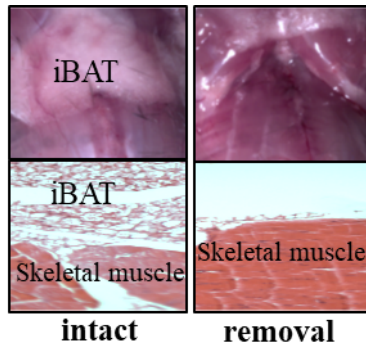


SUPPLEMENTAL MATERIAL

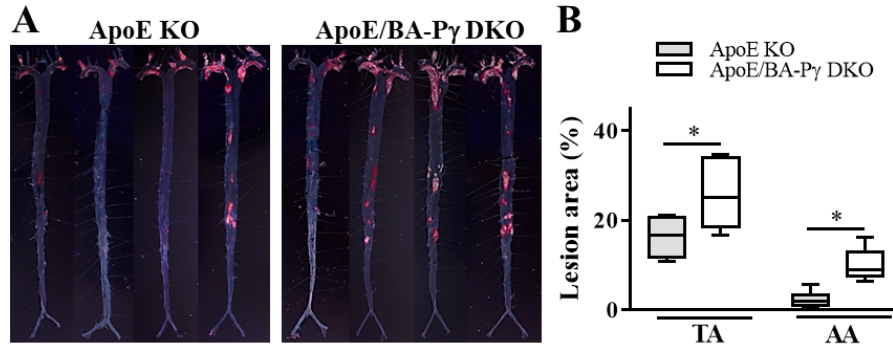
Supplemental Figures and Figure Legends



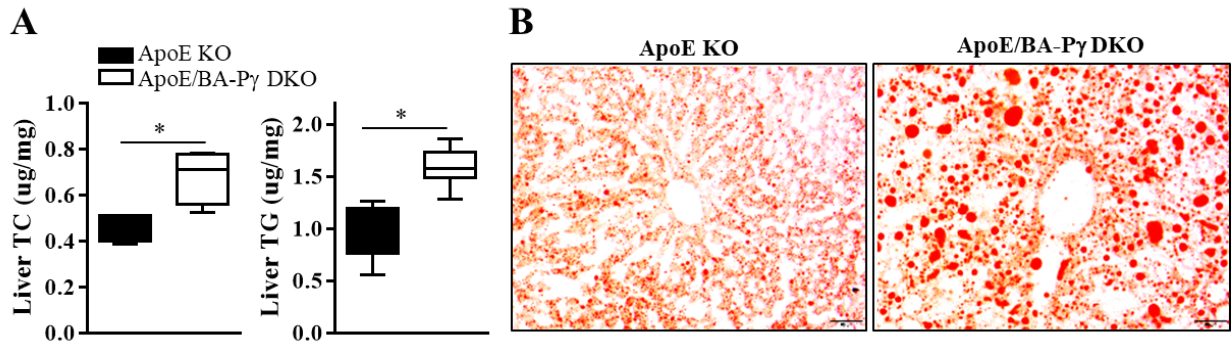
Supplemental Figure I. Characteristics of BA-PPAR γ KO mice. (A). PPAR γ , PPAR α , and PPAR δ mRNA levels in subcutaneous white adipose tissue (sWAT) and gonadal white adipose tissue (gWAT) of male wild type and BA-PPAR γ KO mice. The mRNA levels are expressed relative to 18S. Data shown are mean \pm SD. n=5 mice/group. **p<0.01 vs wild type. (B) Representative digital pictures showing absence of suprarenal abdominal PVAT (aPVAT), normal sWAT and gWAT in BA-PPAR γ KO mice.



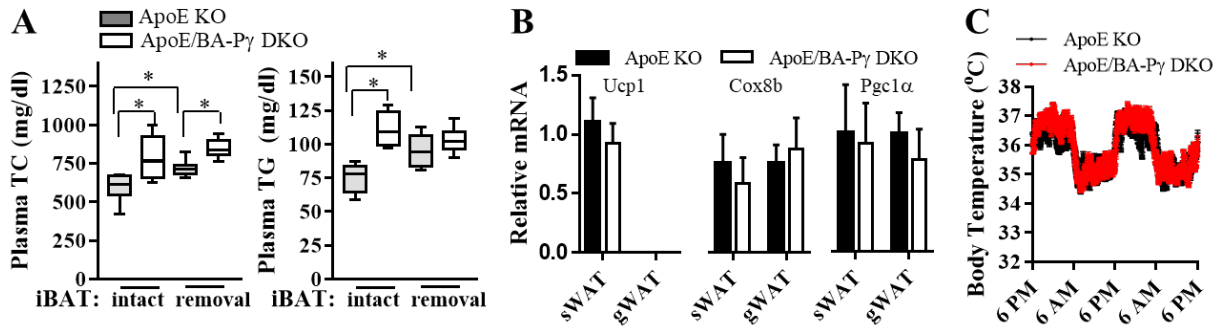
Supplemental Figure II. Representative photographs of iBAT of mice before (intact) and 2 months after surgical removal of iBAT (upper panel) and H.E. staining (lower panel), showing that there was no regeneration of brown adipocyte tissue (lower panel).



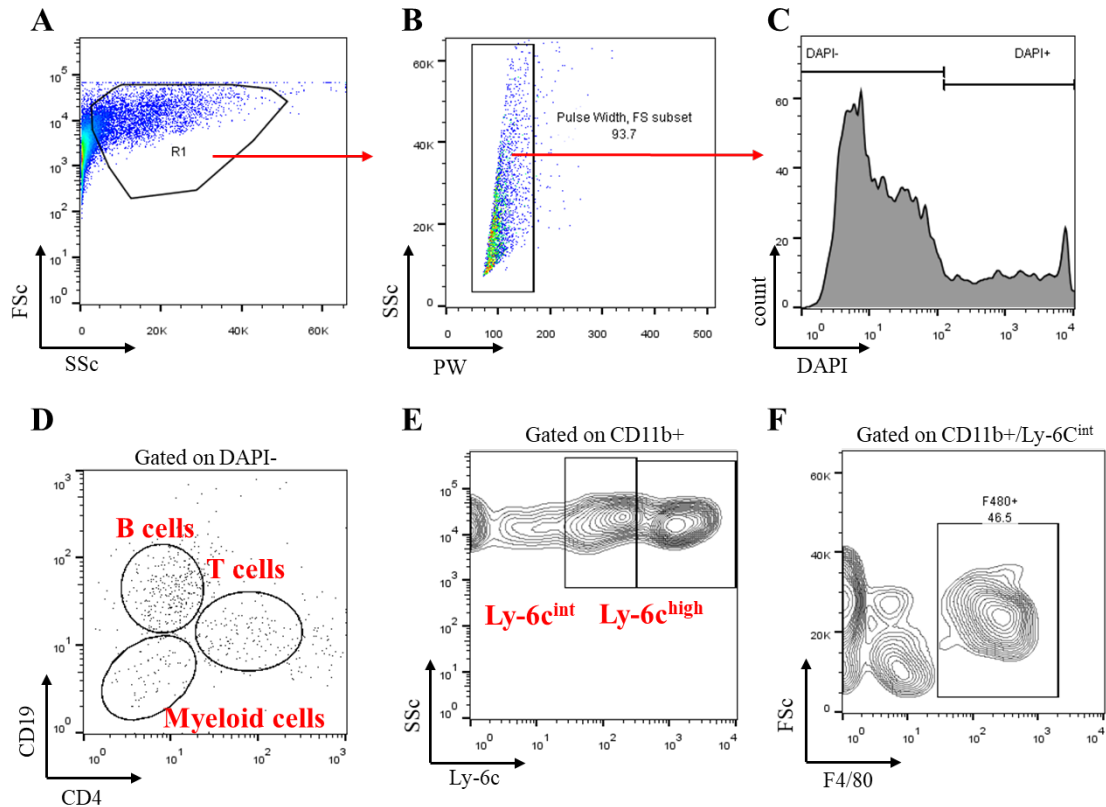
Supplemental Figure III. (A) Eight-week-old female ApoE KO (n=8) and ApoE/BA-PPAR γ KO (n=6) mice were fed a high cholesterol diet for 3 months. Representative Oil Red O staining showing atherosclerotic lesions in the whole aortic trees, and (B) quantitative analysis of the ratio of atherosclerotic lesion area relative to thoracic aorta (TA) and abdominal aorta (AA) total area, respectively. * p <0.05 vs ApoE KO group.



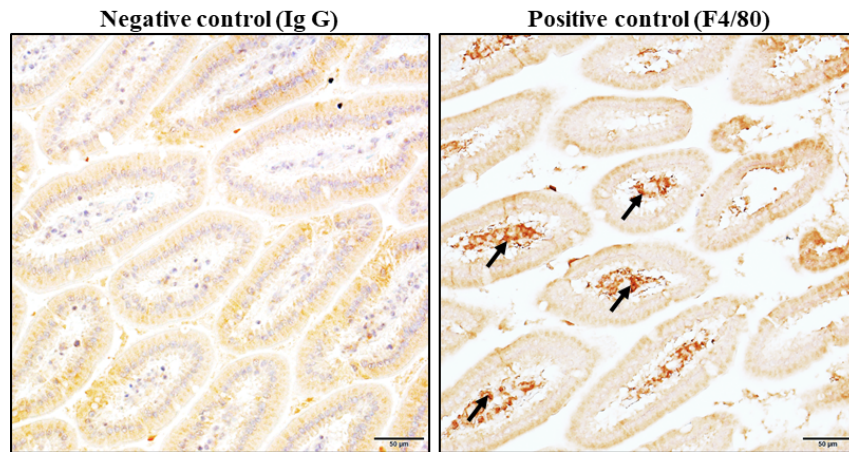
Supplemental Figure IV. (A) Total cholesterol (TC) and triglyceride (TG) levels in the liver of 6-month old male ApoE KO and ApoE/BA-PPAR γ KO mice fed normal chow diet. n=5 mice in ApoE KO group, and n=6 mice in ApoE/BA-P γ DKO group. * p <0.05 vs ApoE KO group. (B) Representative photograph of Oil Red O staining of livers from ApoE KO and ApoE/BA-PPAR γ KO mice after 3-months high cholesterol diet feeding.



Supplemental Figure V. (A) Total cholesterol (TC) and triglyceride (TG) levels in plasma of the ApoE KO and ApoE/BA-PPAR γ KO mice after 2-months on the high cholesterol diet feeding. The iBAT was surgically removed 1-week before starting the high cholesterol diet challenge, n=6 in each group. (B) *Ucp1*, *Cox8b* and *Pgc1 α* mRNA levels in subcutaneous white adipose tissue (sWAT) and gonadal white adipose tissue (gWAT) of the mice in A. The mRNA levels are expressed relative to 18S. Data shown as mean \pm SD. n=3 mice/group. (C) The core body temperature of mice in A measured by radiotelemetry. Data shown as mean \pm SD. n=3 mice/group. No significant differences were found upon analysis.



Supplemental Figure VI: Gating strategy for flow cytometry analysis of PVAT inflammatory cells. **A)** PVAT leukocytes were identified by sequential gating based on **B)** Sizing (Pulse width versus side scatter (SSc); **C)** Exclusion of death or dying cells (DAPI positive). **D)** DAPI negative cells were further gated and defined as B cells CD19+, T cells, CD4+; and myeloid cells as CD11b+, **E)** including monocytes (Ly-6C^{high}) and **F)** macrophages (F4/80+, Ly-6C^{int}).



Supplemental Figure VII: Immunohistological staining for the macrophage marker F4/80. Negative (Ig G) and positive control (F4/80 staining) corresponding to Figure 4B and Figure 6A. Arrows denote positive F4/80 immunoreactivity. Bars indicate 50 µm.